Accepted Manuscript

Mussel-inspired injectable hydrogel and its counterpart for actuating proliferation and neuronal differentiation of retinal progenitor cells

Zhimin Tang, Fang Jiang, Yuanhao Zhang, Yi Zhang, YuanYang, Xiaolin Huang, Yuyao Wang, Dandan Zhang, Ni Ni, Feng Liu, Min Luo, Xianqun Fan, Weian Zhang, Ping Gu

PII: S0142-9612(18)30843-3

DOI: https://doi.org/10.1016/j.biomaterials.2018.12.015

Reference: JBMT 19016

To appear in: *Biomaterials*

Received Date: 28 July 2018

Revised Date: 11 December 2018

Accepted Date: 14 December 2018

Please cite this article as: Tang Z, Jiang F, Zhang Y, Zhang Y, YuanYang , Huang X, Wang Y, Zhang D, Ni N, Liu F, Luo M, Fan X, Zhang W, Gu P, Mussel-inspired injectable hydrogel and its counterpart for actuating proliferation and neuronal differentiation of retinal progenitor cells, *Biomaterials* (2019), doi: https://doi.org/10.1016/j.biomaterials.2018.12.015.

Mussel-inspired injectable hydrogel and its counterpart for actuating proliferation and neuronal differentiation of retinal progenitor cells

Zhimin Tang[1, 2#], Fang Jiang[3#], Yuanhao Zhang[3#], Yi Zhang[1, 2], YuanYang[1, 2], Xiaolin Huang[1, 2], Yuyao Wang[1, 2], Dandan Zhang[1, 2], Ni Ni[1, 2], Feng Liu[3], Min Luo[1, 2], Xianqun Fan[1, 2]*, Weian Zhang[3]*, Ping Gu[1, 2]*

[1] Department of Ophthalmology, Ninth People's Hospital, Shanghai Jiao Tong University School of Medicine, Shanghai, 200011, P.R. China

[2] Shanghai Key Laboratory of Orbital Diseases and Ocular Oncology, Shanghai, 200011, P.R. China

[3] Shanghai Key Laboratory of Functional Materials Chemistry, East China University of Science and Technology, Shanghai, 200237, P. R. China

# These authors contributed equally to this work.

Corresponding Author:

Ping Gu, guping2009@126.com

Weian Zhang, wazhang@ecust.edu.cn

Xianqun Fan, drfanxianqun@126.com

Abstract

Biomaterials-mediated retinal progenitor cell (RPC)-based transplantation therapy has shown substantial potential for retinal degeneration (RD), but it is limited by the poor RPC survival, proliferation and differentiation. Herein, the gelatin-hyaluronic acid (Gel-HA)-based hydrogels formed *via* moderate Michael-type addition reaction with or without the introduction of mussel-inspired polydopamine (PDA), i.e. Gel-HA-PDA and its counterpart Gel-HA hydrogels are developed, and their effects on the biological behaviour of RPCs, including adhesion, survival, proliferation, differentiation, delivery and migration are investigated. The hybrid hydrogels can adopt the intricate structure of the retina with suitable mechanical strength, degradation rate and biological activity to support cellular adhesion, survival and delivery. Meanwhile, Gel-HA hydrogel can remarkably promote RPC proliferation with much larger cell clusters, while Gel-HA-PDA hydrogel significantly enhances RPC adhesion and migration, and directs RPCs to preferentially differentiate toward retinal neurons such as photoreceptors (the most crucial cell-type for RD treatment), which is mainly induced by the activation of integrin α5β1-phosphatidylinositol-3-kinase (PI3K) pathway. This study demonstrates that Gel-HA hydrogel possesses great potential for RPC proliferation, while mussel-inspired PDA-modified Gel-HA hydrogel with superior biocompatibility can significantly promote RPC neuronal differentiation, providing new insights for developing biomedical materials applied for RPC-based transplantation therapy.

Keywords

Hydrogel; Retinal progenitor cells; Polydopamine; Proliferation; Differentiation

1. Introduction

Retinal degeneration (RD), including age-related macular degeneration and retinitis pigmentosa, is the principal cause of irreversible blindness and affects millions world-wide [1]. Several strategies, such as gene therapy, pharmacological treatments, and cell transplantation therapy have been proposed to prevent or retard it. Among them, retinal progenitor cell (RPC)-based transplantation therapy has been brought into focus for sight restoration since RPCs were discovered in the adult mammalian eye and successfully isolated from the human retina [2-4]. Previous studies demonstrated that partial rescue of the deterioration of visual function in different animal models with RD could be achieved by RPC transplantation without ethical concerns and tumorigenicity [5, 6]. However, the limited capacity of RPCs to proliferate and differentiate toward retinal neurons, like photoreceptors, hinders their future clinical applicability [7]. Scientists have made much effort to address the critical issues, including improving the RPC isolation methods, changing the culture media, and the application of culturing carriers [8-10]. Although the culturing carriers, such as poly(1,3-propylene sebacate) and poly(glycerol-sebacate) composites can enhance mouse RPC proliferation as evidenced by the increased expression of proliferation markers [10, 11], these solid scaffolds usually result in poor cell survival associated with subretinal delivery because they lack the flexibility required for the delivery and do not match the modulus of retina [12]. Alternatively, injectable hydrogels, inherently containing hydrous and porous networks, are able to influence stem cell fate, such as proliferation and differentiation, and can serve as a protective

carrier to deliver cells to the expected location with a minimally invasive procedure [13].

One of the basic goals of hydrogel applications in biomedical fields is to mimic native extracellular matrix (ECM) characteristics and intrinsic tissue functions to support cell growth and proliferation. Gelatin, as a hydrolyzed product of collagen, is capable of enhancing proliferation of many cell types, like embryonic stem cells, induced pluripotent stem cells and neural stem cells (NSCs) [13, 14]. Nevertheless, it may not be the superior ECM to mimic retina microenvironment for RPC growth and survival. Another excellent biopolymer hyaluronic acid (HA) has been widely applied in tissue engineering for bone, cartilage and nerve regeneration because of its obviously excellent properties, including good biocompatibility, high hydrophilicity and low immunogenicity [15-17]. It is worth mentioning that HA is a primary constituent present in the subretinal location and can serve as the optimal natural ECM components of retina [18]. The two natural polymers with these ideal characteristics above are attractive in the production of hybrid injectable hydrogels which can not only mimic the ECM microenvironment of retina, but also better support the survival and proliferation of RPCs. In order to achieve a mild chemical reaction in the favored cellular environment, we fabricated a Gel-HA hydrogel by taking full advantages of the moderate Michael-type addition reaction between thiolated gelatin (Gel-SH) and methacrylated hyaluronic acid (HAMA).

Besides, there is still a challenge for biocompatible hydrogels to meet the requirements for inducing the differentiation of RPCs into neurons for vision

restoration. The biological environment of hydrogels has a significant effect on cell differentiation, which is closely related to the adhesion properties of materials [19]. Compared with the traditional hydrogels, hydrogels modified with functional attachment proteins or micromolecules are more beneficial for guiding stem cell adhesion and differentiation [19, 20]. Polydopamine (PDA), inspired by a strong attachment protein in mussel adhesive pads, has been found being responsible for enhancing neurite outgrowth and guiding neuronal development [21, 22]. Hong *et al.* revealed that the oxidation induced dopamine-modified HA hydrogel could enhance cell adhesion and provide high compatibility for encapsulated NSCs [23]. Recently, dopamine-based gelatin methacrylate hydrogels have been shown to promote neuronal differentiation of NSCs [24]. It is worth noting that the retina belongs to the central nervous system, and RPCs possess a multipotency similar to NSCs, indicating that PDA might have a similar positive effect on RPC behaviors such as cell adhesion and differentiation. Herein, Gel-HA-PDA hydrogel was developed by introducing PDA into the Gel-HA precursor solution by crosslinking with covalent and noncovalent bonds with the purpose to study the regulatory properties of the Gel-HA-PDA hydrogel on the differentiation of RPCs and to further investigate the related mechanisms.

In this study, the mussel-inspired Gel-HA-PDA hydrogel and its counterpart Gel-HA hydrogel were developed and evaluated by comprehensive experiments of their mechanical and physicochemical properties. Systematic assessments were conducted to determine the effects of the hydrogels on RPC adhesion, survival, proliferation and

differentiation *in vitro*, and further elucidate the underlying mechanism related to RPC differentiation toward retinal neurons. Moreover, the *in vivo* biocompatibility of the Gel-HA-PDA hydrogel was also evaluated. Based on these evaluations, the hybrid injectable hydrogels represent a promising biomaterial platform for future RPC-based transplantation therapy for RD.

2. Results

2.1. Preparation and characterization of Gel-HA and Gel-HA-PDA hydrogels

Gel-HA hydrogel was successfully fabricated via Michael-type addition reaction between Gel-SH and HAMA in physiological conditions (**Fig. 1**a, **Supplementary Fig. 1**). PDA containing catechol, quinone, and aminos groups noncovalently cross-linked with abundant hydrophilic groups in Gel-SH, and HAMA was utilized to further develop the Gel-HA-PDA hydrogel (**Fig. 1a**) [25]. The ^{1}H-NMR spectra (**Supplementary Fig. 2**) revealed the appearance of a methylene proton peak at δ 2.3 ppm of Gel-COOH due to the ring-opening reaction of succinic anhydride and gelatin. Compared with Gel-COOH, new methylene proton peaks (δ 2.7 ppm, δ 3.2 ppm) were observed after Gel-SH was obtained. According to TNBS (2,4,6-trinitro-benzenesulfonic acid) assays (**Supplementary Fig. 3**) [26], the absorbance at 420 nm indicated that the amount of amine groups decreased obviously after grafting the carboxyl groups. The free thiol group in Gel-SH was 220.98±27.28 μmol g^{-1} determined by Ellman's assay) [27]. HAMA was analyzed by the ^{1}H-NMR spectrum (**Supplementary Fig. 4**), and around 50% modification of HAMA could be obtained by calculation of the integral intensities of two methacrylate proton peaks at δ 5.61 and δ 6.05 (as shown with ″a″) relative to the methyl proton peak at δ 1.9 (as shown with ″b″). Additionally, PDA was formed via dopamine pre oxidation for 48 h, as indicated by a new peak appearing at 420 nm in **Supplementary Fig. 5** [28]. The white Gel-HA and grey Gel-HA-PDA viscous

precursor solutions were injectable by the 26G syringe needle and then formed gels under physiological conditions (**Fig. 1**b**, Supplementary Fig. 6**). The remarkable gray appearance of the Gel-HA-PDA hydrogel was the consequence of the introduced PDA. Scanning electron microscopy (SEM) images as shown in **Fig. 1**c suggested that both hydrogels presented interconnected pores, and the porosity of the lyophilized Gel-HA-PDA hydrogel slightly shrank to a smaller pore size compared with that of the Gel-HA hydrogel. The addition of PDA was also confirmed by BCA assay to quantify the catechol (**Fig. 1**d), which leaded to a significantly increased absorption in the Gel-HA-PDA hydrogel in contrast to the Gel-HA hydrogel.

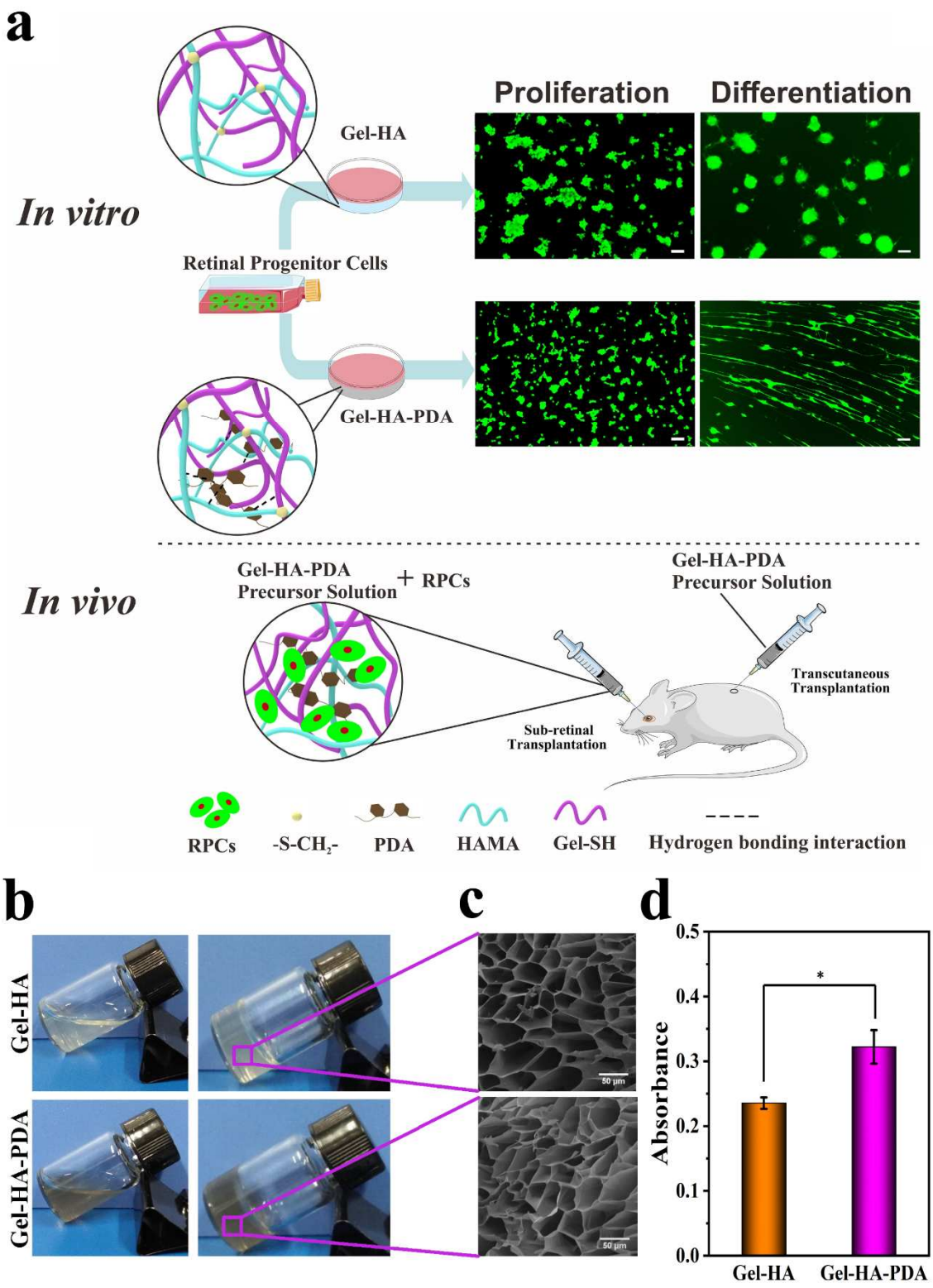

Fig. 1. Schematic and morphology characterization of Gel-HA and Gel-HA-PDA hydrogels. a) Schematic illustration and applications of Gel-HA and Gel-HA-PDA hydrogels. Gel-HA hydrogel improved RPC proliferation, while Gel-HA-PDA hydrogel significantly promoted RPC neuronal differentiation i*n vitro*. *In vivo* studies, the transcutaneous injection of

Gel-HA-PDA hydrogel and subretinal transplantation of GFP^+ RPCs-embedded Gel-HA-PDA hydrogel were conducted. b) The materials gelled under physiological conditions. c) SEM images of hydrogels. d) Confirmation of the presence of PDA in the Gel-HA-PDA hydrogel by analyzing catechol contents using BCA assay. (*$P < 0.05$. Scale bars: 100 μm for (a), 50 μm for (c). Error bars represent the standard deviation of the mean, n=3 independent experiments).

Rheological tests were conducted to analyze the gelation process and viscoelasticity of the hydrogels. As shown in **Fig. 2**a, the gelation time of Gel-HA and Gel-HA-PDA hydrogels was approximately 5 minutes, where the storage modulus (G′) was equal to the loss modulus (G″) (G′= G″). In **Fig. 2**b, the dependence of G′ and G″ on strain amplitude indicated that G′ was not changed in the linear viscoelastic regime (<100% strain), but G′ clearly decreased and G″ increased simultaneously when a higher strain was exerted on the hydrogels, which was caused by the collapse of the crosslinked structure of the hydrogels. Additionally, the hydrogels remained a constant G′ and G″ regardless of the shear frequency ranging from of 0.1-100 rad s^{-1}, indicating the formation of a stable network structure (**Fig. 2**c). From the above rheological tests, the Gel-HA-PDA hydrogel almost had a similar rheological behavior to the Gel-HA hydrogel, except for its slightly lower storage modulus, indicating that the introduction of PDA did not have a great impact on the mechanical properties relative to the Gel-HA hydrogel. Compression tests (**Fig. 2**d) were also performed to evaluate the compressive strength of hydrogels. With the increase of compression ratio, the Gel-HA hydrogel presented a slightly higher compression modulus than the Gel-HA-PDA hydrogel, which is in agreement with the

results of the rheological test. Additionally, both hydrogels showed a high swelling ratio, where the Gel-HA hydrogel and Gel-HA-PDA hydrogel was 27.7 ± 3.2 and 29.9 ± 2.1, respectively (**Fig. 2**e). The biodegradable hydrogels is profound for the generation of new ECM or tissue *in vivo* [29]. Here, about 40% of the hydrogel was degraded in the first 2 h and almost completely degraded within 12 h in the present of collagenase and hyaluronidase *in vitro* (**Fig. 2**f). Cells preferentially differentiate into distinct cell-types when they cultured on ECM with the mechanical stiffness similar to that of the respective *in vivo* tissue [13]. Compared with the native stiffness of retina ECM, the soft injectable hydrogels (about 800 Pa) (**Supplementary Table 1**) well match the modulus of the retina (300–800 Pa) [30]. Moreover, the components of hydrogels developed here mainly consisted of the majority of collagen and HA, which well mimic the native components of retina that includes a bulk of collagen and HA [31]. In general, Gel-HA and Gel-HA-PDA hydrogels exhibited proper mechanical and physicochemical properties, including easy injectability, high porosity, low mechanical strength and excellent biodegradability (**Supplementary Table 1**), indicating their potential applications for RPC-based transplantation therapy for RD.

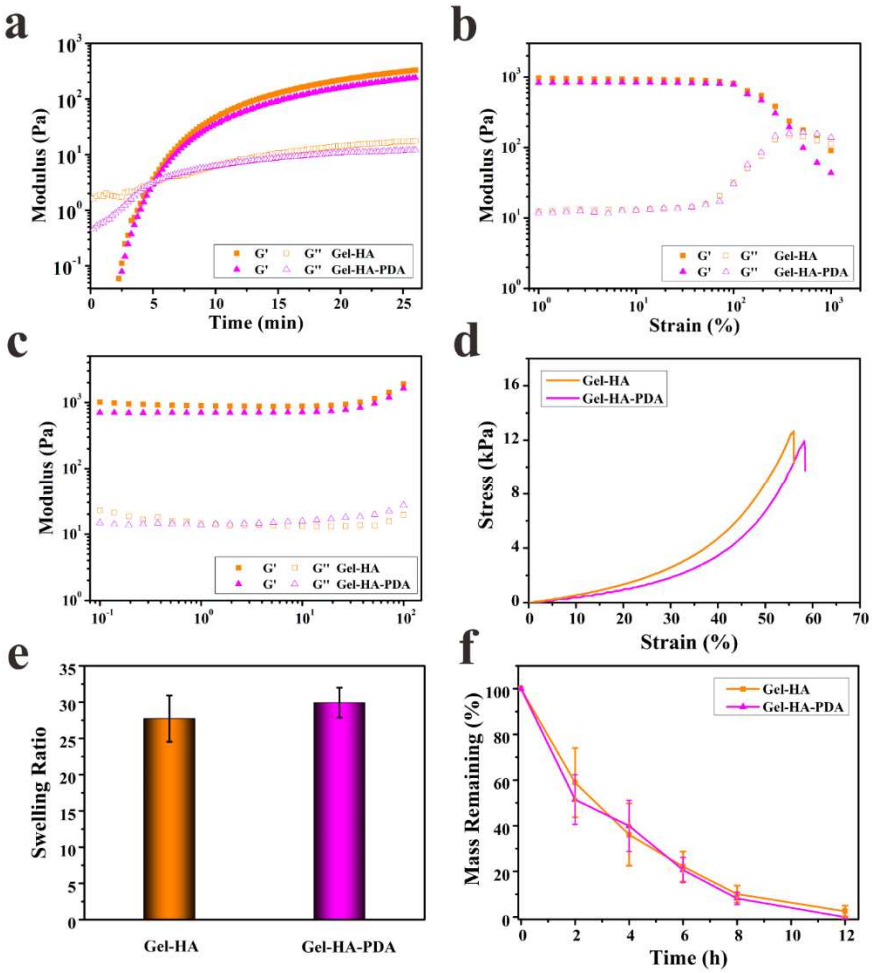

Fig. 2. Mechanical and physiochemical properties of Gel-HA and Gel-HA-PDA hydrogels. Rheological tests of a) time sweep, the gelation time of Gel-HA and Gel-HA-PDA hydrogels was approximately 5 min (G′= G″), b) strain amplitude sweep under a frequency of 1Hz, and c) frequency sweep with the strain of 1%. d) Compressive stress-strain curves. e) Both hydrogels showed a high swelling ratio, and the ratio for Gel-HA hydrogel was 27.7 ± 3.2, and the ratio for Gel-HA-PDA hydrogel was 29.9 ± 2.1. f) *In vitro* biodegradation of hydrogels. Approximately 40% of the hydrogels were degraded in the first 2 h and hydrogels almost completely degraded within 12 h in the present of collagenase and hyaluronidase. (The error bars represent the standard deviation of the mean for n=3 independent experiments.)

2.2. *In vitro* cytocompatibility and cell delivery properties of hydrogels

Specific markers of retinal progenitor cells were analyzed by flow cytometry and

immunostaining (**Supplementary Fig. 7**). High expression levels of retinal progenitor-related markers including Nestin (90.6%), Vimentin (92.2%) and Pax-6 (96.8%) were observed in the cell cultures under proliferation conditions, but only few of glial cell marker GFAP-positive cells (0.5%) and none of retinal ganglion cell (RGC) markers HuD-, Brn-3b- and Thy 1.1-positive cells were detected, indicating that the separated cells were almost retinal progenitor cells, which is consistent with previous studies [32-34]. In addition, the physiological function of RPCs was evaluated by glutamate-evoked calcium response [35]. As presented in **Supplementary Fig. 8** and **Supplementary video 1** and **2**, after glutamate exposure, the RPCs showed a clearly elevated fluorescent intensity in spike amplitude compared with the the adipose-derived stem cells (ADSCs) (negative control). In addition, the time response to peak fluorescence intensity in control ADSCs was also significantly delayed (295 ± 5 sec) in contrast to that in the RPCs group (110 ± 5 sec), suggesting that these cells exhibited RPC specific physiological function.

Live/dead staining, the determination of the expression levels of inflammatory and apoptotic factors, and cell adhesion analysis were conducted to assess the cytocompatibility of hybrid Gel-HA and Gel-HA-PDA hydrogels. Our data showed that RPCs were more than 94% viable on hydrogel substrates after incubation for one day (**Fig. 3**a, b). Injectable hydrogels with cell delivery property can carry donor cells into target sites and exhibit promise for retinal tissue engineering [36]. To evaluate the cell delivery property of injectable hydrogels *in vitro*, the injection of RPCs either with or without hydrogels using 26-gauge needles was performed (**Fig.**

3c). Three hours after injection, the morphology of injected RPCs (injection group) was unchanged compared with that of noninjected RPCs incubated for 3 h (no injection group), and the cell viability of injected RPCs with hydrogels was clearly improved relative to that of the injected RPCs in medium without hydrogels (**Fig. 3**d, e). In comparison with the control, the expression levels of MCP-1 (linked with intraocular inflammatory diseases [37]), IL-6 (a pro-inflammatory cytokine), and Caspase-3 (an important apoptotic factor [38]) dramatically decreased on the hydrogel substrates (**Fig. 3**f-h). In terms of RPC adhesion, the gene expression levels of Cadherin 4, which indicates cell adhesion ability, increased by 40% on the Gel-HA-PDA hydrogel relative to the control, and there were no significant differences between Gel-HA hydrogel and control (**Fig. 3**f). After eliminating non-adherent cells with PBS at 12 h, the number of adherent cells remaining on Gel-HA-PDA hydrogel was greater than that on the untreated control, while the Gel-HA hydrogel showed similar adhesion rate as the control (**Fig. 3**i). Representative fluorescence images of remaining RPCs after washing with PBS showed a higher percentage of remaining RPCs (approximately 73%) on Gel-HA-PDA hydrogel than other groups (approximately 28%) (**Fig. 3**j), further indicated that Gel-HA-PDA hydrogel provided a more attractive environment for RPC adhesion. Overall, our data suggested that the Gel-HA and Gel-HA-PDA hydrogels possess excellent cytocompatibility for RPC adhesion, survival and delivery.

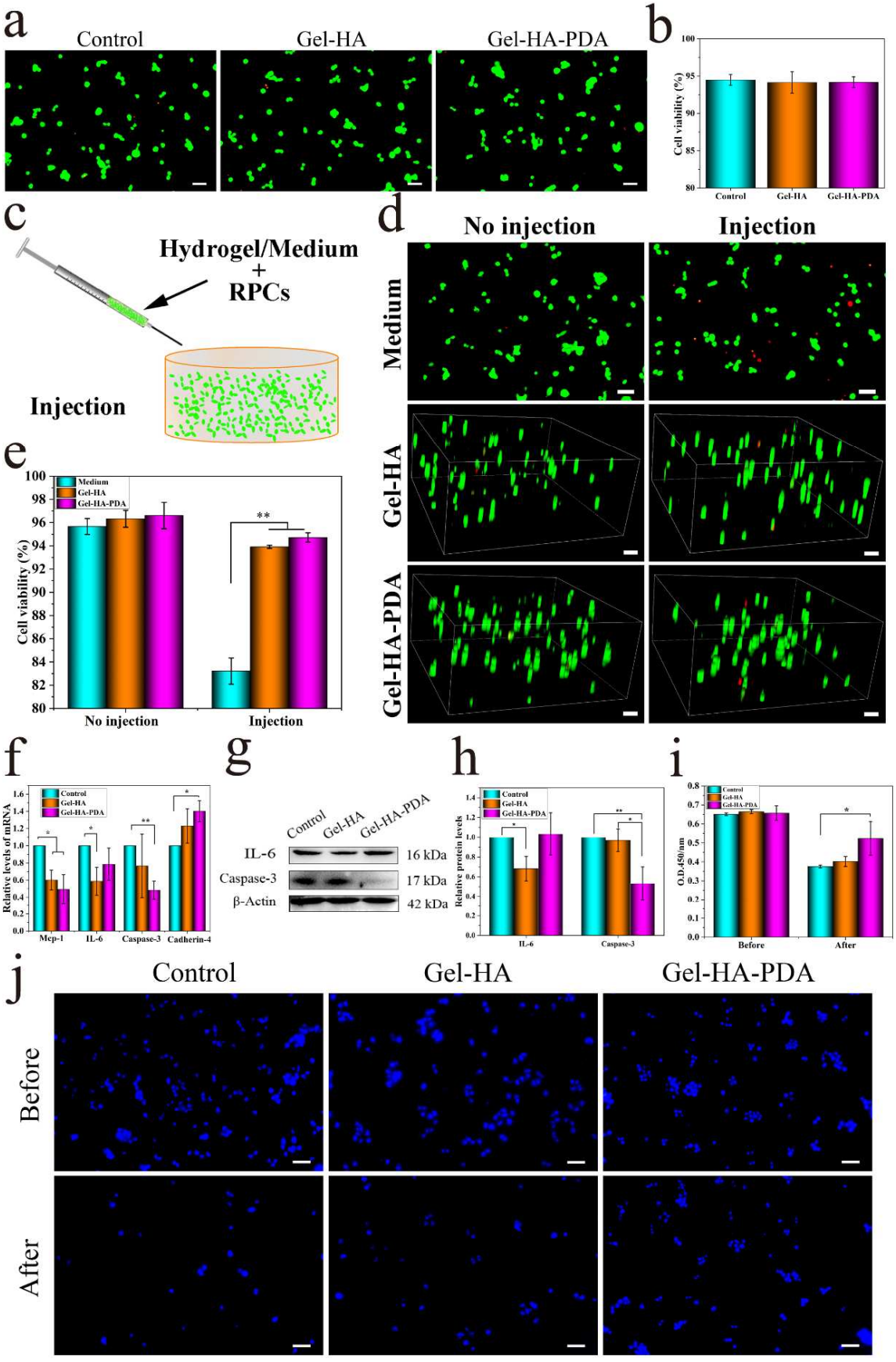

Fig. 3. Cytocompatibility and cell delivery property of Gel-HA and Gel-HA-PDA hydrogels

under proliferation conditions. a) Live/dead staining showed that b) RPCs were more than 94% viable on hydrogel substrates after incubation for one day. c) A schematic illustration of the injection of RPCs either with or without hydrogels using 26-gauge needles. d) Compared with noninjected RPCs incubated for 3 h (no injection), the morphologies of injected RPCs were unchanged 3 h after injection. Live: green, dead: red. e) In the injection group, the viability of RPCs with hydrogels was clearly improved relative to RPCs in medium without hydrogels. f) The gene expression levels of inflammatory factors (IL-6 and MCP-1) decreased in cells on Gel-HA hydrogel, and MCP-1 and apoptotic factor Caspase-3 were downregulated in cells on the Gel-HA-PDA hydrogel compared with cells on tissue culture-treated polystyrene substrates (TCPS), suggesting that the hydrogels possessed excellent cytocompatibility. Additionally, the adhesion factor Cadherin 4 was upregulated on Gel-HA-PDA hydrogel. g) The protein expression levels and h) quantitative analysis of IL-6 and Caspase-3 normalized to β-actin. The cell adhesion ability was further analyzed by i) CCK-8 test and j) fluorescence micrographs of DAPI-stained adherent RPC nuclei at 12 h before and after washing with PBS. Representative fluorescence images of remaining RPCs after washing with PBS showed a higher percentage of remaining RPCs (approximately 73%) on Gel-HA-PDA hydrogel than other groups (approximately 28%), suggesting that the adhesion ability of RPCs cultured on Gel-HA-PDA hydrogel was improved compared with TCPS. (*$P < 0.05$, **$P < 0.01$. Scale bars: 50 μm. The error bars represent the standard deviation of the mean for n=3 independent experiments. The TCPS was control group.).

2.3. Gel-HA hydrogel enhanced proliferation of RPCs

The proliferation capacity of RPCs on Gel-HA and Gel-HA-PDA hydrogels was evaluated by morphologies, qPCR, immunostaining and western blot analyses after three days of incubation. As shown in **Fig. 4**a, the GFP^+ RPCs on Gel-HA hydrogel expanded well with much larger cell clusters, and the cell density of RPCs was dramatically higher than those on the Gel-HA-PDA hydrogel and control. CCK-8 data showed that the RPC expansion capability was promoted at day two and day three on

the Gel-HA hydrogel and was almost equal between the Gel-HA-PDA hydrogel and control (**Fig. 4**b). Moreover, gene expression levels of the cell proliferation marker Ki-67 as well as retinal progenitor-related markers Nestin, Vimentin and Pax-6 were nearly unchanged on the Gel-HA-PDA hydrogel, but markedly upregulated on the Gel-HA hydrogel compared with control (**Fig. 4**c), which were consistent with the results of western blot analysis (**Fig. 4**d,e). Additionally, the percentages of immunoreactive cells for Edu (65.51% vs. 41.47%), Ki-67 (89.04 % vs. 54.66%), Nestin (95.70% vs. 80.00%), and Vimentin (93.33% vs. 80.89%) significantly increased on the Gel-HA hydrogel, and similar outcomes between the Gel-HA-PDA hydrogel and control were presented (**Fig. 4**f, g), as further evidenced by the vast majority of RPCs stained with Edu in 3D Gel-HA hydrogel (**Fig. 4**h). In general, the proliferation ability of RPCs was significantly enhanced in the Gel-HA hydrogel, which is beneficial for the production of sufficient cell sources for RPC-based transplantation therapy.

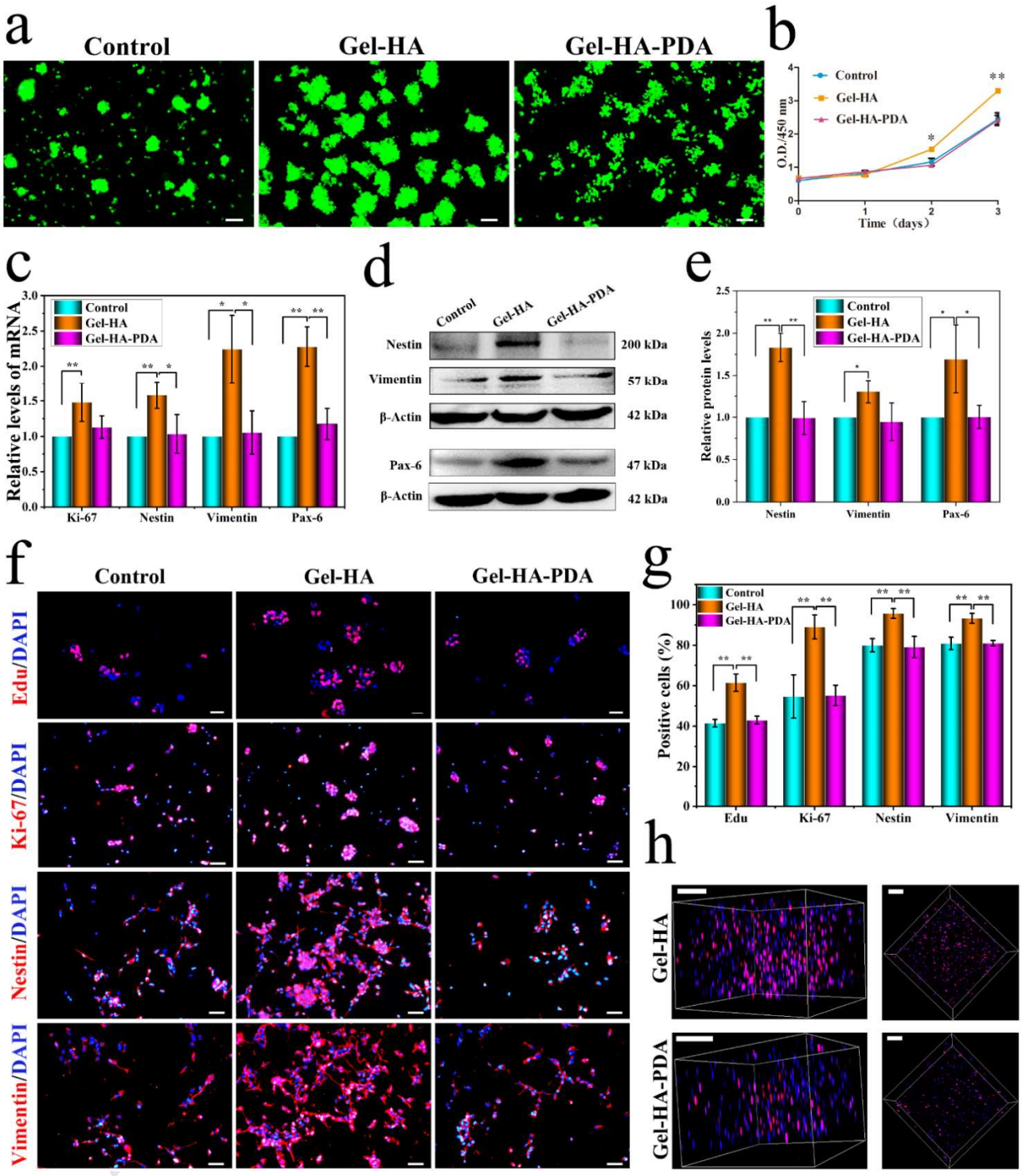

Fig. 4. Evaluation of RPC proliferation in response to Gel-HA and Gel-HA-PDA hydrogels after 3 days of proliferation culture. a) Fluorescent micrographs of GFP^{+} RPCs. The highest cell density was observed in Gel-HA hydrogel. b) The proliferation ability of RPCs detected by a CCK8 assay on Gel-HA hydrogel was markedly enhanced compared with those of other groups after culture for 2 and 3 days. c) The mRNA expression levels of a cell proliferation marker (Ki-67) and retinal progenitor-related markers (Nestin, Vimentin and

Pax-6) were significantly upregulated in cells on Gel-HA hydrogel relative to those in the control group. d) The protein expression levels and e) the quantitative analysis of Nestin, Vimentin and Pax-6 significantly increased on Gel-HA hydrogel in contrast to control. f) Immunostaining with antibodies against Edu, Ki-67, Nestin and Vimentin, and g) quantitative analyses showed that the percentages of marker-positive RPCs on Gel-HA hydrogel were significantly greater than those of other groups. h) Edu staining of RPCs in 3D hydrogels. (*P < 0.05, **P < 0.01, Scale bar: 100 μm for (a) and (h), 50 μm for (f). The error bars represent the standard deviation of the mean for n=3 independent experiments. The TCPS was control group).

2.4. Gel-HA-PDA hydrogel promoted retinal neuronal differentiation of RPCs

To investigate whether the Gel-HA and/or Gel-HA-PDA hydrogel affected neuronal network formation, the divergent morphologies, gene and protein expression levels of RPCs under differentiation culture for 7 days were evaluated. Interestingly, RPCs grown on the Gel-HA hydrogel and control extended only short and thick neurites, whereas the majority of RPCs displayed dramatically longer and thinner neurites on the Gel-HA-PDA hydrogel by further analysis of neurite length (**Fig. 5**a, b). The upregulated gene expression levels of retinal neuron markers, including β3-tubulin, Recoverin (photoreceptor marker) and Pkc-α (bipolar cell marker), and downregulated retinal glia marker GFAP in RPCs cultured on Gel-HA-PDA hydrogel implied that the Gel-HA-PDA hydrogel significantly augmented RPC retinal neuronal differentiation (**Fig. 5**c). Similar stimulating neuronal expression profiles of RPCs cultured with Gel-HA-PDA hydrogel were additionally observed by their respective immunostaining (**Fig. 5**d, e). For example, the Gel-HA-PDA group displayed substantially higher percentages of Recoverin-positive cells (18.12% vs. 9.86%) than the control. The western blot analysis (**Fig. 5**f, g) further supported the Gel-HA-PDA

promoting RPC retinal neuronal differentiation. Herein, both gene and protein expression levels of those markers above were approximately similar between the Gel-HA hydrogel and control. Additionally, cell migration and integration assays were also conducted *in vitro* (**Supplementary Fig. 10**). Our data showed that the improved migration and integration abilities of RPCs were achieved affected by the Gel-HA-PDA hydrogel. Collectively, these data demonstrated that Gel-HA-PDA hydrogel could robustly accelerate RPC commitment to the retinal neuron fate, such as photoreceptors, which is the most crucial cell type for RD treatment.

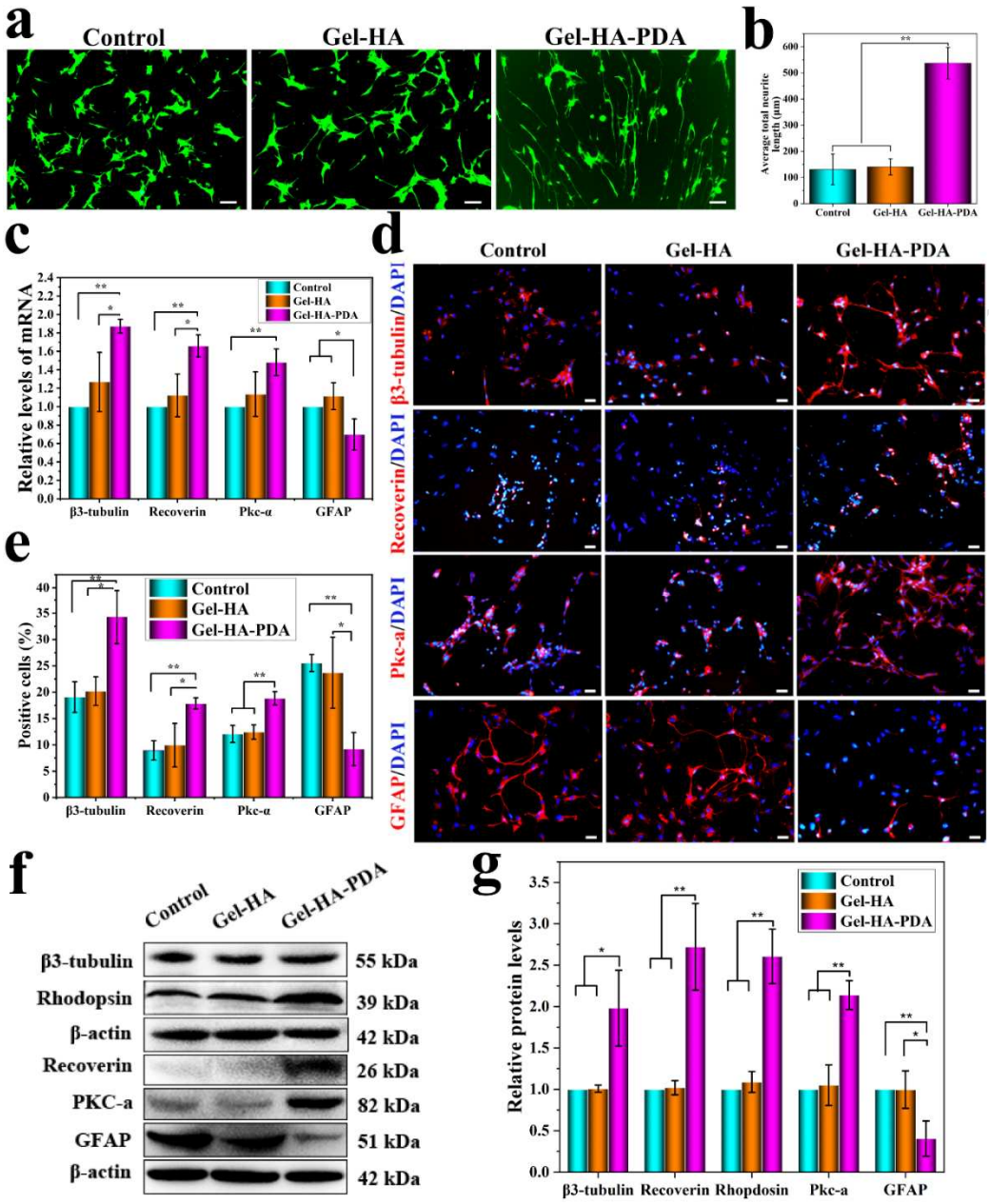

Fig. 5. RPC differentiation affected by Gel-HA-PDA hydrogel after 7 days of differentiation. a) Divergent morphologies and b) quantification of average neurite length of differentiated RPCs (n=6 independent experiments). RPCs grown on Gel-HA-PDA hydrogel mostly exhibited extended and thin neurite-like processes. c) The qPCR results suggested that the mRNA expression levels of β3-tubulin (retinal neuronal cell marker), Recoverin (photoreceptor marker) and Pkc-α (bipolar cell marker) in cells on Gel-HA-PDA hydrogel were substantially upregulated in contrast to the control TCPS group, while GFAP (a retinal glial marker) was downregulated. d) Immunostaining with antibodies against β3-tubulin, Recoverin, Pkc-α and GFAP. e) Quantitative analysis showed that the percentages of

β3-tubulin, Recoverin and Pkc-α-positive cells markedly increased in cells on Gel-HA-PDA hydrogel compared with those in other groups, while the percentages of GFAP-positive cells decreased. f) Protein expression levels and g) quantitative analysis of β3-tubulin, Rhodopsin, Recoverin, Pkc-α and GFAP, normalized to β-actin. (*P < 0.05, **P < 0.01. Scale bars: 100 μm for (a), 50 μm for (d). The error bars represent the standard deviation of the mean for n=3 independent experiments. The TCPS was the control group.).

2.5. Mechanism involved in Gel-HA-PDA hydrogel-induced promotion of retinal neuronal differentiation of RPCs

To better understand the interaction between RPCs and mussel-inspired Gel-HA-PDA hydrogel, we investigated the potential mechanism underlying integrin adhesion receptors (integrin α5β1) and PI3K signaling protein in the RPC neuronal differentiation process that was evoked by the Gel-HA-PDA hydrogel. Herein, the proportions of integrin α5- and PI3K p110γ-positive cells were 3.2-folds and 4.5-folds elevated, respectively, in the cells cultured on the Gel-HA-PDA hydrogel, but integrin β1 exhibited no changes in comparison with the Gel-HA hydrogel and control subjected to immunostaining analysis (**Fig. 6**a,b), which was consistent with the results of western blot analysis (**Fig. 6**c, d). Theoretically, the integrin family could induce the activation of intracellular PI3K, and then the cascades lead to direct cell differentiation [39]. Indeed, the PDA-mediated Gel-HA hydrogel activated PI3K p110γ and that could be abolished by ANT-161 (an antagonist of integrin α5β1) **(Fig. 6**e-g**)**, suggesting an interplay between integrin α5β1 and PI3K signaling. Furthermore, when RPCs were treated with as604850 (an inhibitor of PI3K p110γ), the upregulated protein expression of retinal neuron makers including β3-tubulin,

rhodopsin, and PKC-α in the cells cultured on the Gel-HA-PDA hydrogel was significantly attenuated **(Fig. 6**h-k**)**, further validating that integrin-linked PI3K stimulation was associated with RPC retinal neuronal differentiation affected by the PDA-mediated Gel-HA hydrogel. In summary, our data suggested that the hybrid biopolymer Gel-HA-PDA hydrogel allowed for RPC retinal neuronal differentiation by invoking the integrin family, particularly integrin α5β1, and subsequently activating the PI3K signaling pathway (**Fig. 6**l). Furthermore, a functional assay of RPC neuronal differentiation cultured with Gel-HA-PDA hydrogel upon PI3K signaling modulation was performed by glutamate-evoked calcium response. As shown in **Supplementary Fig. 9** and **Supplementary video 3-6**, after glutamate exposure, an obvious increase of fluorescence intensities was observed in the 740 Y-P (PI3K signaling activator) treatment group (777.75 ± 32.06%) and the Gel-HA-PDA hydrogel group (850.84 ± 98%) in contrast to the TCPS group (540 ± 12.59%), but the as604850 treatment group exhibited a weak signal (**Supplementary Fig. 9**a, b). The response time to the peak fluorescence intensity in as604850-treated cells was significantly delayed (150 ± 5 sec) compared with that of the TCPS group (85 ± 5 sec), and a rapid response time was observed in the 740 Y-P and Gel-HA-PDA hydrogel groups (**Supplementary Fig. 9**c). Glutamate activation has been shown to play an important role in neuronal differentiation in the retina and elsewhere in the central nervous system [35]. These results indicated that PI3K signaling was involved in improving glutamate signaling transmission, and the RPCs cultured with Gel-HA-PDA hydrogel might be programmed to differentiate

into functional neurons by an interaction with PI3K signaling.

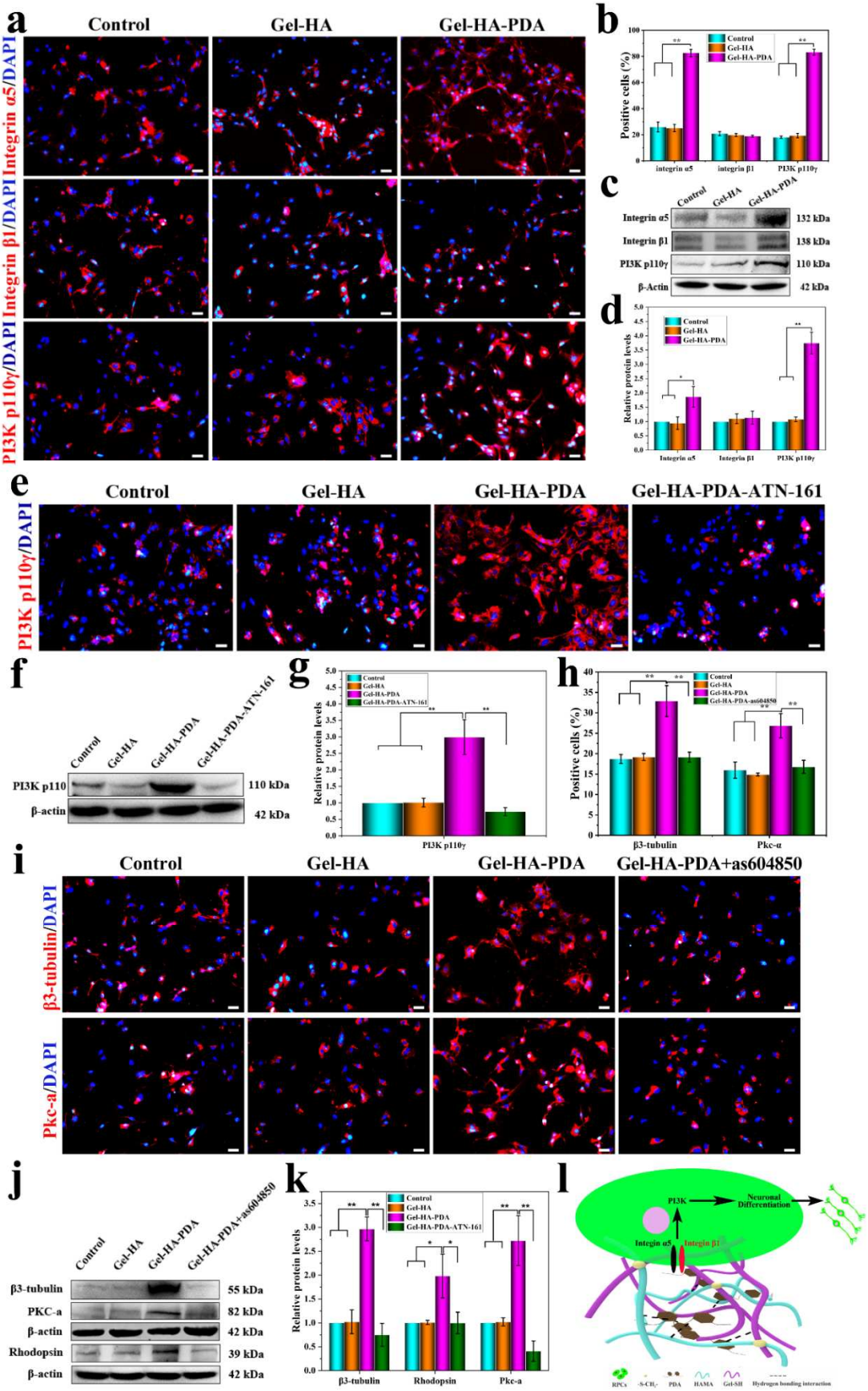

Fig. 6. Interaction between integrin α5β1 and PI3K signaling in RPC neuronal differentiation. a) Immunostaining with antibodies against integrin α5, integrin β1 and PI3K p110γ. b) Quantitative analysis showed that the percentages of integrin α5 and PI3K p110γ-positive cells were markedly upregulated in cells on Gel-HA-PDA hydrogel compared with those in other groups, while the percentages of integrin β1-positive cells were unchanged. c) Protein expression levels and d) quantitative analysis of integrin α5, integrin β1 and PI3K p110γ, normalized to β-actin, showed that the integrin α5 and PI3K were markedly increased, while integrin β1 exhibited no obvious difference compared with those in the control group. The stimulation of PI3K p110γ in Gel-HA-PDA hydrogel was attenuated by ANT-161 (the antagonist of integrin α5β1), *via* e) immunostaining, f) western blot analyses and g) quantitative analysis of PI3K p110γ, normalized to β-actin. h, i) Increased percentages of β3-tubulin and Pkc-α positive cells and j, k) upregulated protein expression levels of β3-tubulin, Rhodopsin and Pkc-α were markedly reduced by as604850 (the inhibitor of PI3K p110γ). l) Hypothesized model of mechanism involves Gel-HA-PDA hydrogel guiding neuronal differentiation of RPCs by activating the integrin α5β1-PI3K signaling pathway. (**P<0.01. Scale bars: 50 μm. The error bars represent the standard deviation of the mean for n=3 independent experiments. The TCPS was the control group.).

2.6. *In vivo* studies of Gel-HA-PDA hydrogel

In order to test tissue biocompatibility, transcutaneous injection of normal saline (control) and Gel-HA-PDA precursor solution without cells in nude mice was performed. A visible gel mass was formed in the subcutaneous space **(Supplementary Fig. 11),** demonstrating it is an in situ-formed hydrogel. The Gel-HA-PDA hydrogel and its surrounding tissue were collected and processed for hematoxylin-eosin (H&E) staining at multiple time points following injection (**Fig. 7**a). No significant inflammatory response was observed on day 3 after implantation. By 7 day, fibroblasts and several inflammatory cells increasingly infiltrated the implant and

were almost localized at the boundary between the hydrogel and surrounding tissue. By days 14 and 21, there were no green-stained CD68-positive macrophages (usually indicating chronic inflammation and excessive foreign body responses), and instead the majority of the fibroblasts that infiltrated into the hydrogel (located below the dotted line) were stained with DAPI at day 14 and marked with white arrows (**Fig. 7**b). Along with the degradation of the Gel-HA-PDA hydrogel up until day 42, i.e., the disappearance of light pink or blue (red arrows) in H&E (**Fig. 7**a) and Masson's trichrome staining (**Fig. 7**c), infiltrating inflammatory cells and fibroblasts were similar to the control, indicating the clearance of hybrid material. In summary, the characteristics and kinetics of tissue reaction to the injected Gel-HA-PDA hydrogel without systemic and chronic inflammations were correlated with the typical foreign body response to implanted material [40, 41].

In addition, the injection of an RPC-embedded Gel-HA-PDA hydrogel into the subretinal space was performed to evaluate the degradability of the hydrogel as well as the migration and integration of transplanted cells, which is a fundamental issue required to be emphasized in RPC-based transplantation therapy [42]. The hydrogel nearly completely degraded within 3 weeks based on OCT scan (**Fig. 7**e) which is a reasonable degraded period for biomaterials *in vivo* [43]. There was no noticeable retinal damage (**Fig. 7**d, e) and no clear increase of inflammatory factor IL-6 positive cells during the entire period (**Supplementary Fig. 12**), demonstrating that the hydrogel possessed good biocompatibility. Importantly, more transplanted GFP^+ RPCs delivered by the Gel-HA-PDA hydrogel appeared in the retinal outer nuclear layer (ONL) at day 7, and cell migration and integration into the inner nuclear layer (INL) at day 14 and into the ganglion cell layer (GCL) at day 21 post implantation were improved compared to the transplanted GFP^+ RPCs delivered by saline (**Fig. 7**f). The decrease of GFP^+ RPC population at day 21 after transplantation was observed

in **Fig. 7**f, which is partly due to the cell migration and dispersion into different retinal layers. In summary, the Gel-HA-PDA hydrogel exhibited an excellent tissue biocompatibility and improved cell migration and integration, which is essential for biomaterial applications in RPC-based transplantation therapy.

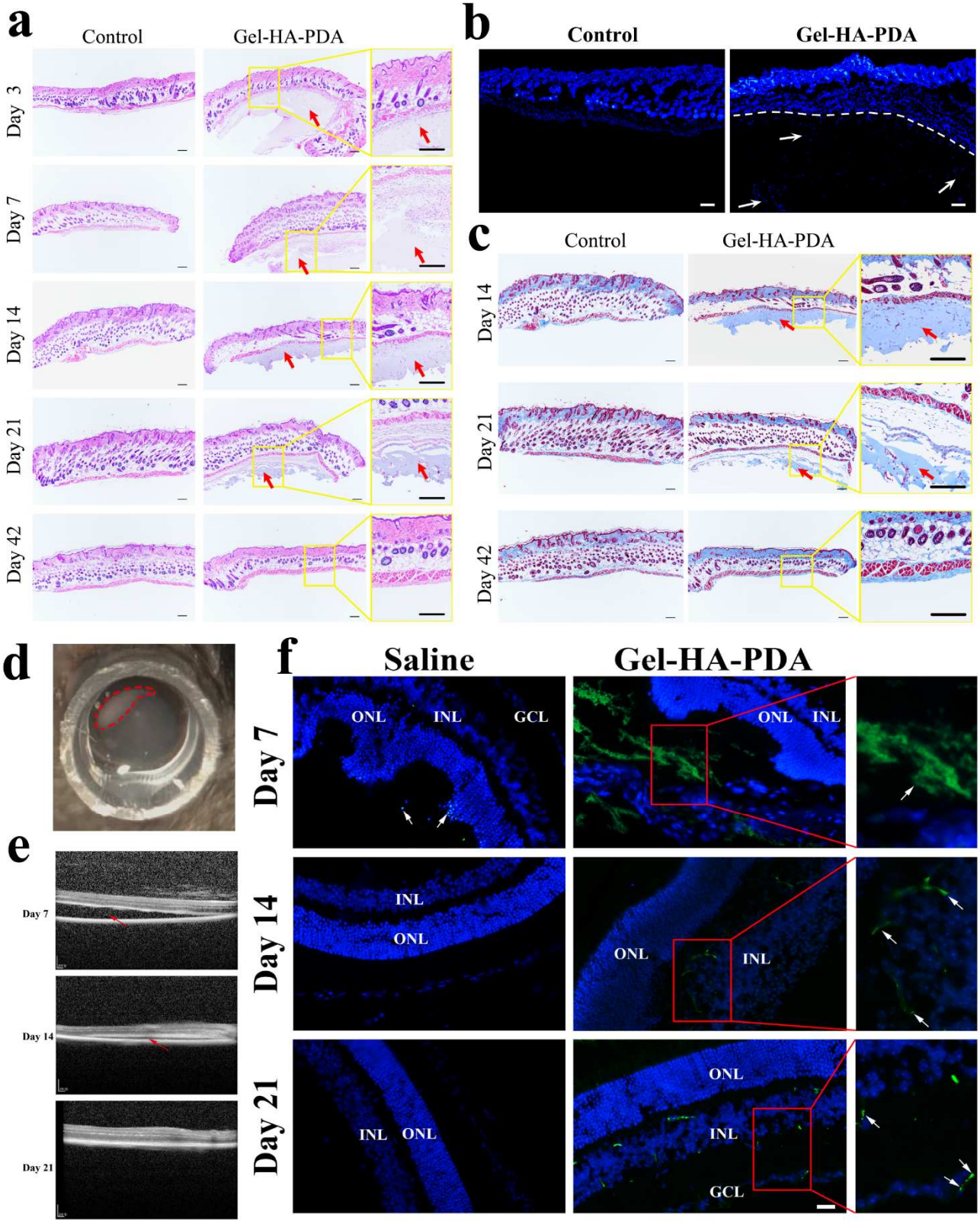

Fig. 7. Transcutaneous biocompatibility of hydrogel and subretinal transplantation of GFP^+ RPC-embedded Gel-HA-PDA hydrogel. a) H&E staining of injected sites and surrounding tissues at days 3, 7, 14, 21, and 42 after implantation. b) $CD68^+$ stained macrophage (green) were not observed in fluorescent images at day 14. Blue nuclei were stained with DAPI. c)

The hydrogel completely degraded within 6 weeks as demonstrated by Masson's trichrome staining. d) Representative images of subretinal transplantation of GFP^+ RPC-embedded Gel-HA-PDA hydrogel by inducing local retinal detachment (as shown with red dotted line). e) Optical coherence tomography (OCT) showed retinal detachment (indicated by red arrow) 1 week after injection, and retinal detachment had largely disappeared 2 weeks following transplantation and an ordered retinal morphology was apparent along with the biomaterial degradation. f) More transplanted GFP^+ RPCs (indicated by white arrows) delivered by Gel-HA-PDA hydrogel appeared in the retinal outer nuclear layer (ONL) at day 7, and migration and integration into the inner nuclear layer (INL) at day 14 and the ganglion cell layer (GCL) at day 21 post implantation were improved compared to transplanted GFP^+ RPCs delivered by saline. (Red arrows in (a) and (c): residual gel, white arrows in (b): infiltrated fibroblasts. Scale bars: 200 μm for (a) and (c) and 50 μm for (f). n=3 independent experiments. The normal saline injection was control group.)

3. Discussion

RD is a serious threat to human vision and no effective treatment has been proposed. Biomaterials-mediated RPC-based transplantation therapy is a promising strategy for the repair of the diseased retina in patients with RD [1, 36]. Choosing a suitable biomaterial which can support RPC survival, proliferation and differentiation as well as facilitate the effective delivery of RPCs to the retinal lesion area is critical for RD treatment. Previous studies have indicated that stiff scaffold biomaterials (>10 kPa), such as poly(sebacoyl diglyceride) and poly(glycerol-sebacate) [10, 11], could play a positive role in RPC proliferation or differentiation to a certain degree, but they usually lack the material flexibility required for the subretinal delivery and do not correspond to the modulus of the retina (300–800 Pa) (300–800 Pa) [30]. Alternatively, soft injectable hydrogels with low Young's modulus, which could better mimic the mechanical properties of soft tissue and allow for minimally invasive administration, are more favorable for retinal regeneration. To the best of our knowledge, few reports have investigated the effects of injectable hydrogels on RPC survival, delivery, proliferation and differentiation. In this study, we fabricated a couple of hybrid injectable hydrogels with excellent cytocompatibility and cell delivery ability for the first time, i.e., mussel-inspired Gel-HA-PDA and its counterpart Gel-HA hydrogels, *via* a feasible and convenient Michael-type addition reaction under mild conditions. Additionally, the Gel-HA hydrogel possesses great potential for RPC proliferation while the PDA-modified Gel-HA hydrogel can significantly promote RPC neuronal differentiation.

The desirable cytocompatibility of hydrogels with low inflammation and apoptosis is helpful for successful cell growth and survival. Herein, the expressions of inflammatory factors and apoptotic factor dramatically decreased with excellent cell survival ability (more than 94%) in our hydrogels. Mitrousis *et al.* reported that HA-based hydrogel possessed the pro-survival effect by deciphering the key mediator mTOR pathway [44], suggesting that similar potential pro-survival mechanisms in our hydrogels. Moreover, gelatin is a biodegradable polymer with excellent biocompatibility and nonantigenicity, and widely applied in biomedical fields [13]. Because of the good biocompatible property of HA and gelatin, a combination of these two modified biopolymers may also have the beneficial effects on cell growth. And the mild Michael-type addition reaction applied herein avoided the potential cytotoxicity caused by other cross-linking methods involving additional catalysts or UV/initiator [45]. Taken together, the data obtained from this study indicate that Gel-HA and Gel-HA-PDA have good cytocompatibility for cell growth and survival, which lays the foundation for RPC proliferation and differentiation.

High efficacy of cell proliferation to obtain abundant transplantable donor cells is an urgent requirement for RPC-based transplantation therapy. In present study, we have observed that the Gel-HA hydrogel markedly enhanced RPC proliferation with much larger cell clusters. As natural biopolymers, Gel-SH and HAMA described herein with similar building blocks to ECM can better mimic retinal niches and provide signals for cell proliferation [14], which is evidenced by the markedly upregulated expressions of the retinal progenitor-related marker Nestin and cell proliferation

marker Ki-67 in the Gel-HA hydrogel. Literatures have indicated that the introduction of biological functional groups, such as amino and carboxyl groups, can promote cell-biomaterial recognition and subsequent proliferation [46]. Therefore, the numerous intrinsic groups, including carboxyl, hydroxyl, and amino groups existed in our polymer chains were contributed to a water-abundant microenvironment for cell proliferation. The micro-environmental mechanical or physical stimuli have been regarded as necessary cues to regulate stem cell fate, including cell growth and proliferation. Our hybrid soft hydrogels with a reasonable stiffness (about 800 Pa) well matched the modulus of retina (300–800 Pa) [30], and presented an interconnected structure with a suitable diameter of 40–50 μm and high porosity (**Supplementary Table 1**), which provide a permissive environment allowing an exchange of nutrients, thereby promoting RPC proliferation. In current study, the Gel-HA hydrogel is beneficial for RPC proliferation, which is important to produce enough door cells for RPC transplantation therapy.

Additionally, RPCs specifically differentiating toward neuronal lineages are further highlighted in RPC-based transplantation therapy. Importantly, the mussel-inspired Gel-HA-PDA hydrogel reported in this study can markedly improve RPC differentiation toward neurons such as photoreceptors, which are one of the most interesting retinal neurons for vision restoration. PDA is known to play a critical role in cell adhesion, and has demonstrated effectiveness in promoting neurite outgrowth and regulating neuronal development [21, 23]. In this study, *in vitro* cell migration and integration assays demonstrated that the improved migration and integration

abilities of RPCs were affected by the mussel-inspired PDA modified Gel-HA-PDA hydrogel, which may result from the strong adhesion property of PDA. In addition, combining a neurotransmitter PDA with a hydrogel may provide a valuable strategy to develop synergistic effects to promote retinal neuron regeneration and further retinal repair. Indeed, the introduction of PDA into Gel-HA hydrogel significantly promoted retinal neuronal differentiation of RPCs, as indicated by the detection of dramatically increased expression levels of retinal neuron-related markers. It has been reported that different dominant functional groups of materials exert various effects on cell fates [47]. For instance, quinone groups that are rich in PDA have been shown to be favorable for cell spreading, and abundant catechol groups on PDA have been shown to affect cell differentiation [48, 49]. In this study, the mussel-inspired PDA-modified Gel-HA hydrogel possessed more catechol groups relative to the Gel-HA hydrogel, which may partly account for the improved retinal neuronal differentiation of RPCs in the Gel-HA-PDA hydrogel. Moreover, the cell adhesive mechanism also plays a crucial role in cell attachment and differentiation processes [50]. We identified the upregulated expression levels of cell adhesion molecule Cadherin 4 and more effective cell attachment to the Gel-HA-PDA hydrogel, which may lay the foundation for cell differentiation. Furthermore, integrin α5β1, a typical adhesive protein of the integrin family, has been shown to direct cell attachment in bioinspired PDA-coated materials and promote cell differentiation by activating the PI3K signaling pathway [51, 52]. As a family of lipid kinases, PI3Ks catalyze the phosphorylation of the cell membrane lipid phosphatidylinositol, which has been proven to be involved in the

promotion of neural differentiation of induced pluripotent stem cells [53]. Consistent with these studies, our data demonstrated that the expression levels of integrin α5- and PI3K p110γ were markedly elevated in cells on the Gel-HA-PDA hydrogel during retinal neuronal differentiation of RPCs, and the inhibition of PI3K (as605048) inhibited the upregulated expression levels of neuronal differentiation markers in RPCs cultured with the Gel-HA-PDA hydrogel. Based on these findings, the mechanism involved in the Gel-HA-PDA hydrogel enhancing RPC commitment to a retinal neuron fate may be related to the stimulation of the integrin α5β1-PI3K pathway. Furthermore, PI3K signaling was involved in improving glutamate signaling transmission, and the RPCs cultured with the Gel-HA-PDA hydrogel might be programmed to differentiate into functional neurons by interactions with PI3K signaling.

In current study, in addition to supporting cell growth and promoting RPC differentiation toward retinal neuronal cells, the Gel-HA-PDA hydrogel displayed excellent tissue biocompatibility *in vivo,* a basic requirement of biomaterials applied for clinical applications, which was achieved by subcutaneous injection of Gel-HA-PDA solution and subretinal injection of RPC-embedded hydrogel. Additionally, the Gel-HA-PDA hydrogel also exhibited a basic property that is required for an ideal cell delivery vehicle applied in the retinal regeneration as follows: the gelation time approximately 5 min can be manipulated to prevent cell loss because rapid gelation may clog the needle during delivery, while a longer gelation time may cause cell backflow and death [43]. Most importantly, the degradation period of the

Gel-HA-PDA hydrogel in the subretinal space was approximately 3 weeks, which may provide a hospitable environment for transplanted cells located in the subretinal space to further migrate and integrate into the retina [43]. Furthermore, the Gel-HA-PDA hydrogel was shown to improve RPC synapse formation by evaluating the expression levels of Synaptophysin *in vitro*. All these data suggest that the PDA-modified Gel-HA hydrogel is a potentially ideal cell carrier for cell survival, neuronal regeneration, delivery, migration and synapse formation, which is an excellent foundation for our future work that will aim to explore the therapeutic effect of Gel-HA-PDA-mediated RPC transplantation therapy, especially the neural re-connection and functional restore, in RD animal models.

Conclusions

This study demonstrated a versatile and novel strategy to construct injectable Gel-HA and Gel-HA-PDA hybrid hydrogels for potential RPC-based transplantation therapy applications. It was demonstrated that both Gel-HA and Gel-HA-PDA hydrogels displayed desirable mechanical properties, excellent biocompatibility and good cell viability after injection, and the Gel-HA hydrogel notably enhanced RPC proliferation to facilitate the production of sufficient transplantable cell sources *in vitro*. Furthermore, the Gel-HA-PDA hydrogel markedly improved RPC attachment and promoted RPC differentiation toward retinal neurons such as photoreceptors (the most crucial cell-type for RD treatment) through the activation of the integrin α5β1-PI3K signaling pathway, indicating that mussel-inspired Gel-HA-PDA and its counterpart Gel-HA hydrogels possess great potential for RPC survival, proliferation, neuronal

differentiation, delivery and migration, which provides new insights for developing biomaterial platform for RPC-based transplantation therapy.

5. Materials and methods

5.1. Materials

Gelatin (Type A, gel strength ~300 g bloom) was purchased from Sigma-Aldrich. Sodium HA (200–400 kD) was bought from Bloomage Freda Biopharm Co., Ltd., China. 2,4,6-trinitro-benzenesulfonic acid (TNBS, 5 w/v% in methyl alcohol) was obtained from Thermo Scientific, USA. Collagenase type I and hyaluronidase were obtained from Yuan Ye biotechnology Co., Ltd., China. All other chemical agents used for materials fabrication were purchased from Aladdin, China. The Cell Counting Kit-8 (CCK8) reagent was purchased from Dojindo China Co., Ltd, China. The Cell Light 5-ethynyl-20-deoxyuridine (Edu) Cell Proliferation Kit was obtained from Guangzhou RiboBio, China. ATN-161 (20 μM, incubation for 30 min) and as-604850 (2.5 μM, treated for 4h) were purchased from Selleck Chemicals. The 740 Y-P (PI3K signaling activator, 100 μg mL^{-1}, and incubation for 48 h) was purchased from Medchemexpress. Unless mentioned otherwise, all cell culture reagents and products were obtained from Invitrogen.

5.2. Preparation of Gel-SH and HAMA

Gel-SH was prepared by two steps based on previous literature [54]. Firstly, gelatin was dissolved in deionized water (100 mL) at 5 wt% for sufficient dissolving. Sequentially, succinic anhydride (7.5 g, 0.075 mol) in acetone (50 mL) was added dropwise to the gelatin solution and maintained at pH=9 using 5 M NaOH for 4 h

reaction. After ending the reaction, the solution was dialyzed against deionized water for 3 days and freeze-dried to gain carboxylated gelatin (Gel-COOH). The substitution from the amino to carboxyl of gelatin was warranted by TNBS assay [26]. Secondly, 1-(3-dimethylaminopropyl)-3-ethylcarbodiimide hydrochloride (EDC) (1.0 g, 5.2 mmol), *N*-hydroxy succinimide (NHS) (0.6 g, 5.2 mmol) and cysteamine hydrochloride (0.4 g, 3.52 mmol) were successively added to the Gel-COOH solution (1.0 g, 100 mL deionized water) and stirred in the dark for 24 h at pH=5.5. The pH of the mixed solution was increased to pH=8.5 with 5M NaOH, followed by adding 1,4-dithio-DLthreitol (DTT) (1.0 g, 6 mmol) for another 24 h reaction. The solution was dialyzed against NaCl solution (pH=3.5, 100 mM) and deionized water for 1 and 2 days separately and freeze-dried. The free thiol groups of Gel-SH were determined by Ellman's assay. HAMA was synthesized according to previous literature [55]. The degree of substitution (DS) was calculated by ^{1}H-NMR analysis (AV 400, Bruker, Germany).

5.3. Formation of injectable Gel-HA and Gel-HA-PDA hydrogels

Gel-SH and HAMA were dissolved in PBS 7.4 at a concentration of 5% (w/v) and 6% (w/v), respectively. They were mixed at the volume ratio of 4:3 to form the Gel-HA hydrogel at 37^{o}C. In regards to the Gel-HA-PDA hydrogel, the solution of PDA was achieved *via* preoxidizing dopamine for 2 days in PBS, and then was added to Gel-HA precursor solution at a final concentration of 0.5 mg mL^{-1}. Furthermore, bicinchoninic acid (BCA) protein assay was performed to quantify the catechol of PDA contained in the Gel-HA-PDA hydrogel according to recommended procedures

[48].

5.4. Scanning electron microscopy (SEM)

The pore size and micromorphology distributions of hydrogels were observed by SEM (VEGA3, TESCAN). Hydrogel samples were freeze-fractured after rapid immersion into liquid nitrogen and lyophilized for 3 days. Then, the fractured surface was coated with a thin layer of gold and observed at an accelerating voltage of 10 kV.

5.5. Mechanical characterization of Gel-HA and Gel-HA-PDA hydrogels

5.5.1. Rheological test

Rheological properties of hydrogels were performed using parallel plate geometry in a Physica MCR 501 rheometer (Anton Paar, Austri) at 37°C in oscillatory mode. The precursor solutions were transferred to the parallel plate and time sweep analysis was carried out at a strain of 1% and an angular frequency of 1 Hz. The gelation time was defined as the storage modulus (G′) equal to the loss modulus (G″) (G′=G″). The molded hydrogels were used for strain (1–1000% strain, 1 Hz) and frequency sweep (0.1–100 rad s^{-1}, 1% strain) analysis equipped with parallel plates of 25 mm diameter and a gap of 1 mm.

5.5.2 Mechanical tests

Mechanical properties were evaluated in a uniaxial compression system (GT-TCS2000, GOTECH, China) with a loading capacity of 100 N. The hydrogel samples were molded as a cylindrical shape at a diameter of 10 mm and thickness of 9 mm. Hydrogels were compressed at the rate of 1 mm min^{-1} until fracture. The compression modulus was further calculated at 10% deformation of initial height.

5.6. Swelling properties and biodegradability *in vitro*

After lyophilization, the hydrogels were immersed into PBS in 12-well plates at 37°C for 48 h for swelling equilibrium (SR) and weighted. The SR was calculated by Equation **(1)**:

$$SR = W_t/W_0 \quad \textbf{(1)}$$

where W_t and W_0 were the weights of the swollen hydrogels in the equilibrium state and dry hydrogels, respectively.

Lyophilized hydrogels were degraded with 2.5 U mL^{-1} collagenase type I and 2.5 U mL^{-1} hyaluronidase in PBS, and shaking at 100 rpm at 37°C. At each predetermined time interval, the hydrogels were rinsed with deionized water to remove the remaining enzyme and freeze-dried again. The residual mass was calculated by Equation **(2)**:

$$\text{residual mass (\%)} = W_m/W_i \times 100\% \quad \textbf{(2)}$$

where W_i was the weight of the initial dry hydrogels and W_m was the dry weight after degradation.

5.7. Isolation and culture of RPCs

The RPCs were separated as previously described [56]. Briefly, they were collected from fresh retinal tissue of postnatal day 1 GFP-transgenic C57BL/6 mice, then were plated on T25 flasks and cultured with proliferation medium in consist of advanced DMEM/F12, 2 mM L-glutamine, 1% N2 neural supplement, 20 ng ml^{-1} epidermal growth factor and 100 U mL^{-1} penicillin-streptomycin [57]. For differentiation study, the RPCs were cultured with differentiation medium that contained 10% fetal bovine serum (FBS) without epidermal growth factor.

Different morphologies of GFP^+ RPCs seeded on a 6-cm dish under proliferation conditions for 3 days and differentiation conditions for 7 days were visualized *via* fluorescent microscope (Nikon). Tissue culture-treated polystyrene substrates (TCPS) served as a control. The neurite length of differentiated RPCs on hydrogel substrates was tested and quantified by ImageJ analysis software (NIH, MD).

Isolated GFP^+ cells were characterized by detecting the expression levels of retinal progenitor-related markers Nestin, Vimentin and Pax-6, as well as the glial cell marker GFAP using flow cytometry (BD Bioscience) [33] and immunostaining (as described below). The percentages of these positive markers in GFP^+ cells detected by flow cytometry were calculated with respect to isotype control cells.

5.8. Live/dead assay

RPCs cultured with hydrogels in 24-well plates (4×10^4 cells $well^{-1}$) were stained using a live/dead kit according to recommended procedures. For 2D culture, each well was gelled with 15 μL Gel-HA or Gel-HA-PDA hydrogel filtered prior to use. For 3D culture, single cell suspensions of RPCs were mixed with 70 μL Gel-HA or Gel-HA-PDA precursor solution per well. To test the cell delivery ability of hydrogels, the cell viability in the 3D hydrogels and proliferation medium (control) was further analyzed and divided into two groups. The no injection group was incubated directly for 3 h, and the injection group was injected using a 26-gauge and then incubated for 3 h supplemented with an additional 400 μL proliferation medium into each well. After treatment of live/dead kit for 30 min, the images were taken by fluorescence microscope and laser scanning microscopy (Nikon). Live and dead RPCs were

counted by ImageJ software, and cell viability was calculated as (live cells/total cells in the field) ×100%.

5.9. CCK-8 assay

A CCK-8 kit was utilized to evaluate RPC proliferation (1×10^4 cells per well) and adhesion abilities (2×10^4 cells per well) in 96-well plate. Each well was coated with 10 μL Gel-HA or Gel-HA-PDA hydrogel. The proliferation capability of RPCs was evaluated using CCK-8 solution (10 μL $well^{-1}$) at 0, 1, 2, and 3 days. After centrifuging this plate for 4 min, the supernatant (170 μL) was pipetted into one new 96-well plate. To test cell adhesion, unattached RPCs were removed from the substrates by washing with PBS at 12 h after seeding, and the remaining RPCs were incubated with CCK8. An ELISA microplate reader (ELX800, BioTeK, USA) was employed to measure optical density at 450 nm. After that, the nuclei before and after washing with PBS were stained with 4, 6 diamidino-2-phenylindole (DAPI), and imaged by a fluorescent microscope (Nikon). The percentage of remaining RPCs after washing with PBS was calculated as follows: (remaining RPCs after washing with PBS/total RPCs before washing with PBS in the field of view) ×100%.

5.10. Edu assay

Edu reagent was added to react with proliferating cells cultured with 2D and 3D hydrogels according to recommended procedures. After discarding Edu medium mixture, RPCs were fixed with 4% paraformaldehyde (PFA) for 30 min and stained with Apollo Dye Solution, and then nucleic acids were stained with Hoechst 33342 for 30 min. Photographs were taken by fluorescent microscope and laser scanning

microscopy (Nikon). The cell proliferation ratio was the (Edu add-in cells/Hoechst stained cells in the field) ×100%.

5.11. RNA extraction and quantitative polymerase chain reaction (qPCR)

The quantified RPCs (2×10^5 cell ml^{-1}) were seeded on 6-well plates coated with 60 μL Gel-HA or Gel-HA-PDA hydrogel per well, then were cultured for 7 days (differentiation condition) or 3 days (proliferation condition). Total RNA was harvested using TRIzol reagent according to manufacturer's instructions. The qPCR was carried out by Real-Time PCR Detection System (Applied Biosystems, Foster, CA) to detect the mRNA expression levels of Ki-67, Nestin, Vimentin and Pax-6 to determine the proliferation and stemness ability of RPCs. The gene expression of Pkc-α, β3-tubulin, Recoverin and GFAP were analyzed to investigate RPC differentiation ability. The primers and parameters were listed in **Supplementary Table 2.** Data normalized to the gene expression of β-actin were analyzed as fold change relative to control.

5.12. Immunostaining

Immunostaining was conducted to investigate RPC proliferation (3 days) and differentiation (7 days) ability in 24-well plates. At determined time, they were fixed with 4% PFA and blocked with blocking solution (TBS containing 0.3% Triton X-100 and 10% normal goat serum (Sigma-Aldrich)). The cells were incubated with rabbit monoclonal anti-Vimentin (Epitomics, 1:200), Recoverin (Millipore, 1:200), Synaptophysin and Pax-6 (Abcam, 1:200), and mouse monoclonal anti-HuD, Brn-3b (Santa Cruz Biotechnology, 1:100), Thy 1.1 (Millipore, 1:200), Nestin, Ki-67, Pkc-α

(BD Biosciences, 1:200), β3-tubulin, GFAP (Chemicon, 1:200), PI3K p110γ, integrin α5 and integrin β1 (Santa Cruz Biotechnology, 1:100) at 4 °C overnight. Then they were labeled with secondary antibodies (Alexa Fluor 546 goat anti-mouse or rabbit IgG, BD Biosciences, 1:800). Finally, cell nuclei were counterstained with DAPI and observed by fluorescent microscope (Olympus BX51, Japan). ImageJ software was used to count cells and the positive ratio was calculated with (immunepositive cells/DAPI stained cells in the field) ×100%.

5.13. Western blot analysis

All groups were prepared as previously described in qPCR assay. Total proteins were harvested at 3 day (proliferation culture) or 7 day (differentiation culture) and analyzed by BCA Kit (Pierce, Rockford, IL). Proteins were separated by SDS-PAGE (Bio-red) electrophoresis, then transferred to PVDF membranes (Millipore, Bedford, MA), and incubated with primary antibodies rabbit monoclonal anti-mouse Vimentin, Pax-6, Recoverin (Millipore) and Synaptophysin (Abcam), and mouse monoclonal anti-nestin, Rhodopsin, β3-tubulin, GFAP (Millipore), Pkc-α (BD), PI3K p110γ, integrin α5, integrin β1 (Santa Cruz Biotechnology) and β-actin (Sigma-Aldrich). The horseradish peroxidase-conjugated secondary antibody (Sigma-Aldrich) was utilized and the protein expressions were visualized by ECL Plus Western Blot Detection Kit (Tanton).

5.14. Glutamate-evoked calcium response

Glutamate-evoked calcium response was conducted to evaluate physiological function of separated RPCs under proliferation condition for 3 days, or differentiated RPCs

under differentiation condition for 7 days. Spontaneous intracellular calcium transient was analyzed by Rhod-2-acetoxymethyl ester (Rhod-2 AM).There were two groups cultured under proliferation condition: 1) RPCs and 2) negative control adipose-derived stem cells (ADSCs) isolated and cultured according to previous protocol [58]. Under differentiation condition, four groups were evaluated as follows: 1) TCPS group, 2) Gel-HA-PDA hydrogel group, 3) 740 Y-P (PI3K signaling activator) treatment group, and 4) as604850 (PI3K signaling inhibitor) treatment group. At a determined time point, RPCs were incubated in Hanks' balanced salt solution (HBSS, Ca^{2+}/Mg^{2+}-free; Gibco) containing 4 μM Rhod-2 AM and 0.1% pluronic F-127 for 20 min at 37°C. Then cells were washed with HBSS, and 10 μM glutamate (Sigma-Aldrich) was added. A fluorescence microscope (Nikon) was immediately used to acquire images with an excitation wavelength of 550 nm and an emission wavelength of 576 nm. The fluorescence intensity at specific time intervals was measured on a total of 50 cells in triplicate experiments. The cellular change in fluorescence (F; %ΔF/Fbaseline) of each region was calculated as follows: (Ftreated – Fbaseline)/Fbaseline ×100%.

5.15. Cell migration assays

RPCs at a density of $3x10^5$ cells/well were seeded on 6‑well plates either coated with or without the Gel-HA-PDA hydrogel and grown into monolayers under differentiation medium. Upon reaching 95% confluence, the cell monolayer was scraped by a 200 μL pipette tip to generate scratch wounds. The cells were washed with PBS to remove floating debris and the width of the wound was photographed at

0 h, 36 h and 72 h.

5.16. Subcutaneous injection of Gel-HA-PDA hydrogel without cells and subretinal injection of RPCs-embedded Gel-HA-PDA hydrogel

Gel-HA-PDA hydrogel was prepared in DMEM-F12 medium. All 30 nude mice (4 weeks of age, 12±2 g) were randomly divided into two groups: control (saline injection) and Gel-HA-PDA hydrogel without cells. Each side of the dorsal region of every mouse was subcutaneously implanted with 100 μL saline or Gel-HA-PDA polymer solution with a 26 G syringe needle at room temperature. Three mice in each group were sacrificed at 3, 7, 14, 21 and 42 day post-injection. Skin around the injected site and residue of the implant were carefully incised and isolated. After that, they were immediately fixed in 10% formaldehyde for H&E and Masson's trichrome staining, and embedded with opti-mum cutting temperature compound for CD68 immunohistochemical staining (Abcam, 1:100). The blocked samples were sectioned in 5 μm consecutive sections, and staining results were observed by light microscope (Nikon).

Subretinal transplantation of the RPC-embedded Gel-HA-PDA hydrogel into a single eye of each mouse was adapted from a previously described technique [36]. Briefly, 28-day-old C57BL/6 wild-type mice were divided into 2 different groups as follows: 1) RPC-embedded saline composites and 2) RPC-embedded Gel-HA-PDA hydrogel composites (1 μL, containing 10,000 cells μL^{-1}), which were injected using a 34-gauge beveled needle through a sclerotomy into the subretinal space between the retinal pigment epithelium and retina. Immunosuppression was not used. The mice

were sacrificed at 7, 14, or 21 days postsurgery, and the eyes were anesthetized for spectral domain optical coherence tomography (SD-OCT; Spectralis, Heidelberg Engineering Inc, Heidelberg, Germany) and harvested for immunofluorescence (IL-6). All experiments conformed to the Association for Research in Vision and Ophthalmology (ARVO) statement and the requirements of the Animal Research Committee of Ninth People's Hospital, Shanghai Jiao Tong University School of Medicine.

5.17. Statistical analysis

All statistics were expressed as mean ± standard deviation (SD) from at least three repeated experiments, and analyzed by Student's t-tests. $P<0.05$ and $P<0.01$ were considered to be statistically significant.

Acknowledgements

The research was supported by the National Natural Science Foundations of China (81570883, 81870687 and 21574039), the National Key R&D program of China (2018YFC1106101), Shanghai Municipal Education Commission-Gaofeng Clinical Medicine Grant Support (20161316) and the Science and Technology Commission of Shanghai (17DZ2260100).

Conflict of Interest

The authors declare no conflict of interest.

Appendix A. Supplementary data

Supplementary data related to this article can be found from the Elsevier Online

Library or from the author.

References

[1] R.R. Bourne, G.A. Stevens, R.A. White, J.L. Smith, S.R. Flaxman, H. Price, J.B. Jonas, J. Keeffe, J. Leasher, K. Naidoo, K. Pesudovs, S. Resnikoff, H.R. Taylor, Causes of vision loss worldwide, 1990-2010: a systematic analysis, Lancet Glob. Health 1(6) (2013) e339-49.

[2] B.G. Ballios, M.J. Cooke, L. Donaldson, Brenda L.K. Coles, C.M. Morshead, D. van der Kooy, M.S. Shoichet, A Hyaluronan-Based Injectable Hydrogel Improves the Survival and Integration of Stem Cell Progeny following Transplantation, Stem Cell Rep. 4(6) (2015) 1031-45.

[3] V. Tropepe, B.L. Coles, B.J. Chiasson, D.J. Horsford, A.J. Elia, R.R. McInnes, D. van der Kooy, Retinal stem cells in the adult mammalian eye, Science 287(5460) (2000) 2032-36.

[4] B.L. Coles, B. Angenieux, T. Inoue, K. Del Rio-Tsonis, J.R. Spence, R.R. McInnes, Y. Arsenijevic, D. van der Kooy, Facile isolation and the characterization of human retinal stem cells, Proc. Natl. Acad. Sci. U. S. A. 101(44) (2004) 15772-77.

[5] S.Y. Li, Z.Q. Yin, S.J. Chen, L.F. Chen, Y. Liu, Rescue from light-induced retinal degeneration by human fetal retinal transplantation in minipigs, Curr. Eye Res. 34(7) (2009) 523-35.

[6] H.J. Klassen, T.F. Ng, Y. Kurimoto, I. Kirov, M. Shatos, P. Coffey, M.J. Young, Multipotent retinal progenitors express developmental markers, differentiate into retinal neurons, and preserve light-mediated behavior, Invest. Ophthalmol. Vis. Sci. 45(11) (2004) 4167-73.

[7] P. Gu, L.J. Harwood, X. Zhang, M. Wylie, W.J. Curry, T. Cogliati, Isolation of retinal progenitor and stem cells from the porcine eye, Mol. Vis. 13 (2007) 1045-57.

[8] P.Y. Baranov, B.A. Tucker, M.J. Young, Low-oxygen culture conditions extend the multipotent properties of human retinal progenitor cells, Tissue Eng., Part A 20(9-10) (2014) 1465-75.

[9] Y. Hu, J. Ji, J. Xia, P. Zhao, X. Fan, Z. Wang, X. Zhou, M. Luo, P. Gu, An in vitro comparison study: the effects of fetal bovine serum concentration on retinal progenitor cell multipotentiality, Neurosci. Lett. 534 (2013) 90-95.

[10] N. Ni, J. Ji, S. Chen, D. Zhang, Z. Wang, B. Shen, C. Guo, Y. Zhang, S. Wang, X. Fan, Z. You, M. Luo, P. Gu, Poly(1,3-propylene sebacate) and Poly(sebacoyl diglyceride): A Pair of Potential Polymers for the Proliferation and Differentiation of Retinal Progenitor Cells, Macromol. Biosci. 16(9) (2016) 1334-47.

[11] S. Redenti, W.L. Neeley, S. Rompani, S. Saigal, J. Yang, H. Klassen, R. Langer, M.J. Young, Engineering retinal progenitor cell and scrollable poly(glycerol-sebacate) composites for expansion and subretinal transplantation, Biomaterials 30(20) (2009) 3405-14.

[12] M. Tomita, E. Lavik, H. Klassen, T. Zahir, R. Langer, M.J. Young, Biodegradable polymer composite grafts promote the survival and differentiation of retinal progenitor cells, Stem Cells 23(10) (2005) 1579-88.

[13] T.C. Tseng, L. Tao, F.Y. Hsieh, Y. Wei, I.M. Chiu, S.H. Hsu, An Injectable, Self-Healing Hydrogel to Repair the Central Nervous System, Adv. Mater. 27(23) (2015) 3518-24.

[14] L. Liu, M. Yoshioka, M. Nakajima, A. Ogasawara, J. Liu, K. Hasegawa, S. Li, J. Zou, N. Nakatsuji, K. Kamei, Y. Chen, Nanofibrous gelatin substrates for long-term expansion of human pluripotent stem cells, Biomaterials 35(24) (2014) 6259-67.

[15] J.M. Townsend, B.T. Andrews, Y. Feng, J. Wang, R.J. Nudo, E. Van Kampen, S.H. Gehrke, C.J. Berkland, M.S. Detamore, Superior calvarial bone regeneration using pentenoate-functionalized hyaluronic acid hydrogels with devitalized tendon particles, Acta Biomater. 71 (2018) 148-55.

[16] A. La Gatta, G. Ricci, A. Stellavato, M. Cammarota, R. Filosa, A. Papa, A. D'Agostino, M. Portaccio, I. Delfino, M. De Rosa, C. Schiraldi, Hyaluronan hydrogels with a low degree of modification as scaffolds for cartilage engineering, Int. J. Biol. Macromol. 103 (2017) 978-89.

[17] M.H. Yang, K.C. Chen, P.W. Chiang, T.W. Chung, W.J. Chen, P.Y. Chu, S.C. Chen, Y.S. Lu, C.H. Yuan, M.C. Wang, C.Y. Lin, Y.F. Huang, S.B. Jong, P.C. Lin, Y.C. Tyan, Proteomic Profiling of Neuroblastoma Cells Adhesion on Hyaluronic Acid-Based Surface for Neural Tissue Engineering, Biomed Res. Int. 2016 (2016) 1917394.

[18] S.J. Clark, T.D. Keenan, H.L. Fielder, L.J. Collinson, R.J. Holley, C.L. Merry, T.H. van Kuppevelt, A.J. Day, P.N. Bishop, Mapping the differential distribution of glycosaminoglycans in the adult human retina, choroid, and sclera, Invest. Ophthalmol. Vis. Sci. 52(9) (2011) 6511-21.

[19] J. Lee, A.A. Abdeen, D. Zhang, K.A. Kilian, Directing stem cell fate on hydrogel substrates by controlling cell geometry, matrix mechanics and adhesion ligand composition, Biomaterials 34(33) (2013) 8140-48.

[20] X. Wang, C. Yan, K. Ye, Y. He, Z. Li, J. Ding, Effect of RGD nanospacing on differentiation of stem cells, Biomaterials 34(12) (2013) 2865-74.

[21] K. Yang, J.S. Lee, J. Kim, Y.B. Lee, H. Shin, S.H. Um, J.B. Kim, K.I. Park, H. Lee, S.W. Cho, Polydopamine-mediated surface modification of scaffold materials for human neural stem cell engineering, Biomaterials 33(29) (2012) 6952-64.

[22] H. Lee, S.M. Dellatore, W.M. Miller, P.B. Messersmith, Mussel-inspired surface chemistry for multifunctional coatings, Science 318(5849) (2007) 426-30.

[23] S. Hong, K. Yang, B. Kang, C. Lee, I.T. Song, E. Byun, K.I. Park, S.W. Cho, H. Lee, Hyaluronic Acid Catechol: A Biopolymer Exhibiting a pH‐Dependent Adhesive or Cohesive Property for Human Neural Stem Cell Engineering, Adv. Funct. Mater. 23(14) (2013) 1856.

[24] X. Zhou, H. Cui, M. Nowicki, S. Miao, S.J. Lee, F. Masood, B.T. Harris, L.G. Zhang, Three-Dimensional-Bioprinted Dopamine-Based Matrix for Promoting Neural Regeneration, ACS Appl. Mater. Interfaces 10(10) (2018) 8993-9001.

[25] L. Han, X. Lu, K. Liu, K. Wang, L. Fang, L.T. Weng, H. Zhang, Y. Tang, F. Ren, C. Zhao, Mussel-Inspired Adhesive and Tough Hydrogel Based on Nanoclay Confined Dopamine Polymerization, ACS Nano 11(3) (2017) 2561.

[26] A.F. Habeeb, Determination of free amino groups in proteins by trinitrobenzenesulfonic acid, Anal. Biochem. 14(3) (1966) 328-36.

[27] J. Rohrer, O. Zupančič, W. Suchaoin, K. Netsomboon, F. Laffleur, S. Oh, A. Bernkop-Schnürch, Synthesis and in vitro characterisation of preactivated thiolated gelatin, Eur. Polym. J. 73 (2015) 268-77.

[28] X. Du, L. Li, J. Li, C. Yang, N. Frenkel, A. Welle, S. Heissler, A. Nefedov, M. Grunze, P.A. Levkin, UV-triggered dopamine polymerization: control of polymerization, surface coating, and photopatterning, Adv. Mater. 26(47) (2014) 8029–33.

[29] G. Camci-Unal, D. Cuttica, N. Annabi, D. Demarchi, A. Khademhosseini, Synthesis and Characterization of Hybrid Hyaluronic Acid-Gelatin Hydrogels, Biomacromolecules 14(4) (2013) 1085.

[30] K. Chen, A.P. Rowley, J.D. Weiland, Elastic properties of porcine ocular posterior soft tissues, J. Biomed. Mater. Res., Part A 93(2) (2010) 634-45.

[31] J. Kundu, A. Michaelson, K. Talbot, P. Baranov, M.J. Young, R.L. Carrier, Decellularized retinal matrix: Natural platforms for human retinal progenitor cell culture, Acta Biomater. 31 (2016)

61-70.

[32] H. Klassen, K. Warfvinge, P.H. Schwartz, J.F. Kiilgaard, N. Shamie, C. Jiang, M. Samuel, E. Scherfig, R.S. Prather, M.J. Young, Isolation of progenitor cells from GFP-transgenic pigs and transplantation to the retina of allorecipients, Cloning and Stem Cells 10(3) (2008) 391-402.

[33] P.Y. Zhou, G.H. Peng, H. Xu, Z.Q. Yin, c-Kit(+) cells isolated from human fetal retinas represent a new population of retinal progenitor cells, J. Cell Sci. 128(11) (2015) 2169-78.

[34] D. Zhang, B. Shen, Y. Zhang, N. Ni, Y. Wang, F. Xianqun, H. Sun, P. Gu, Betacellulin regulates the proliferation and differentiation of retinal progenitor cells in vitro, J. Cell. Mol. Med. 22(1) (2017) 330-45.

[35] W. Sun, G.M. Seigel, R.J. Salvi, Retinal precursor cells express functional ionotropic glutamate and GABA receptors, Neuroreport 13(18) (2002) 2421-24.

[36] B.G. Ballios, M.J. Cooke, D. van der Kooy, M.S. Shoichet, A hydrogel-based stem cell delivery system to treat retinal degenerative diseases, Biomaterials 31(9) (2010) 2555-64.

[37] T. Nakazawa, T. Hisatomi, C. Nakazawa, K. Noda, K. Maruyama, H. She, A. Matsubara, S. Miyahara, S. Nakao, Y. Yin, L. Benowitz, A. Hafezi-Moghadam, J.W. Miller, Monocyte chemoattractant protein 1 mediates retinal detachment-induced photoreceptor apoptosis, Proc. Natl. Acad. Sci. U. S. A. 104(7) (2007) 2425-30.

[38] M. Brentnall, L. Rodriguez-Menocal, R.L. De Guevara, E. Cepero, L.H. Boise, Caspase-9, caspase-3 and caspase-7 have distinct roles during intrinsic apoptosis, BMC Cell Biol. 14 (2013) 32.

[39] J.S. Lee, J.K. Yi, S.Y. An, J.S. Heo, Increased osteogenic differentiation of periodontal ligament stem cells on polydopamine film occurs via activation of integrin and PI3K signaling pathways, Cell. Physiol. Biochem. 34(5) (2014) 1824-34.

[40] J.M. Anderson, A. Rodriguez, D.T. Chang, Foreign body reaction to biomaterials, Semin. Immunol. 20(2) (2008) 86-100.

[41] A.M. Kligman, R.C. Armstrong, Histologic response to intradermal Zyderm and Zyplast (glutaraldehyde cross-linked) collagen in humans, J. Dermatol. Surg. Oncol. 12(4) (1986) 351-57.

[42] D. Singh, S.B. Wang, T. Xia, L. Tainsh, M. Ghiassi-Nejad, T. Xu, S. Peng, R.A. Adelman, L.J. Rizzolo, A biodegradable scaffold enhances differentiation of embryonic stem cells into a thick sheet of retinal cells, Biomaterials 154 (2018) 158-68.

[43] Y. Liu, R. Wang, T.I. Zarembinski, N. Doty, C. Jiang, C. Regatieri, X. Zhang, M.J. Young, The application of hyaluronic acid hydrogels to retinal progenitor cell transplantation, Tissue Eng., Part A 19(1-2) (2013) 135-42.

[44] N. Mitrousis, R.Y. Tam, A.E.G. Baker, V.D.K. Derek, M.S. Shoichet, Hyaluronic Acid‐Based Hydrogels Enable Rod Photoreceptor Survival and Maturation In Vitro through Activation of the mTOR Pathway, Adv. Funct. Mater. 26(12) (2016) 1975-85.

[45] Y.C. Chen, R.Z. Lin, H. Qi, Y. Yang, H. Bae, J.M. Melero-Martin, A. Khademhosseini, Functional Human Vascular Network Generated in Photocrosslinkable Gelatin Methacrylate Hydrogels, Adv. Funct. Mater. 22(10) (2012) 2027-39.

[46] N. Faucheux, R. Schweiss, K. Lutzow, C. Werner, T. Groth, Self-assembled monolayers with different terminating groups as model substrates for cell adhesion studies, Biomaterials 25(14) (2004) 2721-30.

[47] Y.J. Ren, H. Zhang, H. Huang, X.M. Wang, Z.Y. Zhou, F.Z. Cui, Y.H. An, In vitro behavior of neural stem cells in response to different chemical functional groups, Biomaterials 30(6) (2009)

1036-44.

[48] R. Luo, L. Tang, S. Zhong, Z. Yang, J. Wang, Y. Weng, Q. Tu, C. Jiang, N. Huang, In vitro investigation of enhanced hemocompatibility and endothelial cell proliferation associated with quinone-rich polydopamine coating, ACS Appl. Mater. Interfaces 5(5) (2013) 1704-14.

[49] G. Tan, Y. Liu, Y. Wu, K. Ouyang, L. Zhou, P. Yu, J. Liao, C. Ning, Electrically Reversible Redox-Switchable Polydopamine Films for Regulating Cell Behavior, Electrochim. Acta 228 (2017) 343-50.

[50] S.H. Bhang, S.H. Kwon, S. Lee, G.C. Kim, A.M. Han, Y.H. Kwon, B.S. Kim, Enhanced neuronal differentiation of pheochromocytoma 12 cells on polydopamine-modified surface, Biochem. Biophys. Res. Commun. 430(4) (2013) 1294-300.

[51] J.L. Wang, K.F. Ren, H. Chang, F. Jia, B.C. Li, Y. Ji, J. Ji, Direct adhesion of endothelial cells to bioinspired poly(dopamine) coating through endogenous fibronectin and integrin alpha5 beta1, Macromol. Biosci. 13(4) (2013) 483-93.

[52] Z. Hamidouche, O. Fromigue, J. Ringe, T. Haupl, P. Vaudin, J.C. Pages, S. Srouji, E. Livne, P.J. Marie, Priming integrin alpha5 promotes human mesenchymal stromal cell osteoblast differentiation and osteogenesis, Proc. Natl. Acad. Sci. U. S. A. 106(44) (2009) 18587-91.

[53] T. Shu, C. Liu, M. Pang, L. He, B. Yang, L. Fan, S. Zhang, X. Wang, B. Liu, L. Rong, Salvianolic acid B promotes neural differentiation of induced pluripotent stem cells via PI3K/AKT/GSK3beta/beta-catenin pathway, Neurosci. Lett. 671 (2018) 154-60.

[54] G. Xu, X. Wang, C. Deng, X. Teng, E.J. Suuronen, Z. Shen, Z. Zhong, Injectable biodegradable hybrid hydrogels based on thiolated collagen and oligo(acryloyl carbonate)-poly(ethylene glycol)-oligo(acryloyl carbonate) copolymer for functional cardiac regeneration, Acta Biomater. 15 (2014) 55-64.

[55] Y. Zhang, X. Pan, Z. Shi, H. Cai, Sustained release of stem cell factor in a double network hydrogel for ex vivo culture of cord blood-derived CD34(+) cells, Cell Prolif. 51(2) (2018) e12407.

[56] J. Xia, H. Liu, X. Fan, Y. Hu, Y. Zhang, Z. Wang, X. Zhou, M. Luo, P. Gu, An in vitro comparison of two different subpopulations of retinal progenitor cells for self-renewal and multipotentiality, Brain Res. 1433 (2012) 38-46.

[57] P. Gu, J. Yang, J. Wang, M.J. Young, H. Klassen, Sequential changes in the gene expression profile of murine retinal progenitor cells during the induction of differentiation, Mol. Vis. 15 (2009) 2111-22.

[58] Q. Xie, Z. Wang, H. Zhou, Z. Yu, Y. Huang, H. Sun, X. Bi, Y. Wang, W. Shi, P. Gu, X. Fan, The role of miR-135-modified adipose-derived mesenchymal stem cells in bone regeneration, Biomaterials 75 (2016) 279-94.